ChemPubSoc Europe

DOI: 10.1002/cmdc.201900489

CHEMMEDCHEM Full Papers

Molecular Epitope Determination of Aptamer Complexes of the Multidomain Protein C-Met by Proteolytic Affinity-Mass Spectrometry

Loredana Lupu,[a] Pascal Wiegand,[a] Nico Hüttmann,[a, b] Stephan Rawer,[a] Wolfgang Kleinekofort,[a, c] Irina Shugureva,[e, f] Anna S. Kichkailo,[f] Felix N. Tomilin,[d, e] Alexander Lazarev,[g] Maxim V. Berezovski,[b] and Michael Przybylski*[a]

C-Met protein is a glycosylated receptor tyrosine kinase of the hepatocyte growth factor (HGF), composed of an α and a β chain. Upon ligand binding, C-Met transmits intracellular signals by a unique multi-substrate docking site. C-Met can be aberrantly activated leading to tumorigenesis and other diseases, and has been recognized as a biomarker in cancer diagnosis. C-Met aptamers have been recently considered a useful tool for detection of cancer biomarkers. Herein we report a molecular interaction study of human C-Met expressed in kidney cells with two DNA aptamers of 60 and 64 bases (CLN0003 and CLN0004), obtained using the SELEX (**S**ystematic **E**volution of **L**igands by **Ex**ponential Enrichment) procedure. Epitope peptides of aptamer-C-Met complexes were identified by proteolytic affinity-mass spectrometry in combination with SPR biosensor analysis (PROTEX-SPR-MS), using high-pressure proteolysis for efficient digestion. High affinities (K_D, 80–510 nM) were determined for aptamer-C-Met complexes, with two-step binding suggested by kinetic analysis. A linear epitope, C-Met (381–393) was identified for CLN0004, while the CLN0003 aptamer revealed an assembled epitope comprised of two peptide sequences, C-Met (524–543) and C-Met (557–568). Structure modeling of C-Met-aptamers were consistent with the identified epitopes. Specificities and affinities were ascertained by SPR analysis of the synthetic epitope peptides. The high affinities of aptamers to C-Met, and the specific epitopes revealed render them of high interest for cellular diagnostic studies.

Introduction

Structure-function studies of membrane receptor proteins play a key role in approaches to understand the physiological basis for the development of targeted drugs for different diseases, but their molecular mechanisms of interaction are poorly understood. As an example, the characterization of molecular interaction sites of the C-Met protein has received high interest in the study of receptors as possible targets for cancer treatment. C-Met and its corresponding ligand, the hepatocyte growth factor protein (HGF) have been intensively studied as targets for anticancer drugs, and their abnormal activities have been implicated in tumorigenesis.[1–4] C-Met is a glycosylated tyrosine kinase receptor of HGF[5] that consists of a disulfide-linked α/β heterodimer formed by proteolytic processing of a precursor protein in the post-Golgi compartment.[6] The structure of C-Met is comprising two domains, an extracellular α-region (Figure 1) and a transmembrane β-region linked by disulfide bridges. The α-region has three major domains: A Semaphorin (Sema) domain; a plexin-Semaphorin-integrin (PSI) domain; and four immunoglobulin-plexin transcription (IPT) domains.[7] The N-terminal Sema domain encompasses approximately 500 residues and shares sequence homology with domains of the semaphorin and plexin families. The PSI domain of ca. 50 residues is connected to a transmembrane helix via four IPT domains. The extracellular region is responsible for binding to HGF and is composed of the Sema domain, a cysteine-rich Met-related sequence (MRS), and four immunoglo-

[a] L. Lupu, P. Wiegand, N. Hüttmann, S. Rawer, Prof. Dr. W. Kleinekofort, Prof. Dr. M. Przybylski
Steinbeis Centre for Biopolymer Analysis and Biomedical Mass Spectrometry
Marktstraße 29
65428 Rüsselsheim am Main (Germany)
E-mail: michael.przybylski@stw.de
[b] N. Hüttmann, Prof. Dr. M. V. Berezovski
Department of Chemistry and Biomolecular Sciences
University of Ottawa
Ottawa, ON, K1N 6N5 (Canada)
[c] Prof. Dr. W. Kleinekofort
Dept. of Engineering Sciences
Rhein Main University
65428 Rüsselsheim am Main (Germany)
[d] F. N. Tomilin
Kirensky Institute of Physics
Russian Academy of Sciences Siberian Branch
Krasnoyarsk 660036 (Russia)
[e] I. Shugureva, F. N. Tomilin
Siberian Federal University
Krasnoyarsk 66041 (Russia)
[f] I. Shugureva, Dr. A. S. Kichkailo
Federal Research Center "Krasnoyarsk Science Center of the Siberian Branch of the Russian Academy of Science"
Laboratory for Digital Controlled Drugs and Theranostics
Krasnoyarsk 660036 (Russia)
[g] Dr. A. Lazarev
Pressure Biosciences Inc.
14 Norfolk Ave.
South Easton, MA 02375 (USA)

Supporting information for this article is available on the WWW under https://doi.org/10.1002/cmdc.201900489

© 2019 Wiley-VCH Verlag GmbH & Co. KGaA, Weinheim

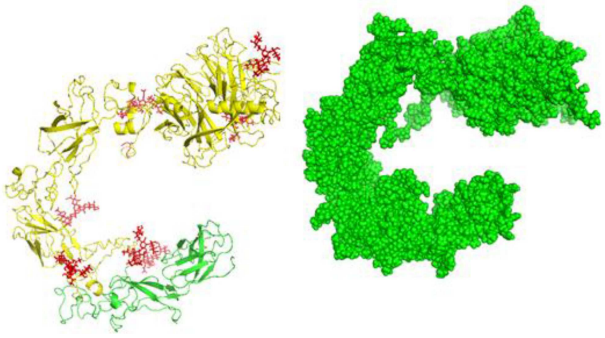

Figure 1. Structure model of the recombinant human C-Met/Fc Chimera protein according to I-TASSER.[36] Highlighted in yellow is the extracellular domain of human c-Met precursor[1–932] and in green the C-terminal polyhistidine-tagged Fc region of human IgG 1 used.

bulin-like structures (IgG domains).[8] The β-region contains a juxtamembrane segment, carboxy-terminal sequences and a tyrosine kinase domain.[3,4,8]

Upon ligand binding and autophosphorylation by a specific multi-substrate docking site, C-Met transmits intercellular signals that are essential for tissue repair, embryonic development, and liver regeneration.[3,4] Conversely, aberrant activation of C-Met can lead to tumorigenesis, schizophrenia and cardiomyocytes.[3] The interaction between C-Met and HGF triggers phosphorylation of two tyrosine residues within the catalytic loop (Tyr-1234; Tyr-1235).[1] Aberrant overexpression of C-Met by interaction with its ligand HGF causes tumor progression.[4,5] Recent studies suggest that within tumor cells, aberrant activation of C-Met by HGF occurs by an autocrine loop. Interaction studies of the signaling pathway of C-Met to HGF are currently ongoing,[1,6] but no molecular mechanism has been hitherto identified.

Several antibodies have been evaluated in the development of inhibitors of the C-Met signaling pathway.[8–10] C-Met inhibiting antibodies have been tested in first clinical trials; some were found to delay tumor progression[9] and have been recently approved by the U.S. Food and Drug Administration for treatment of several types of tumors. First studies to elucidate binding sites of C-Met with inhibiting monoclonal antibodies have been reported.[11] Cao et al.[10] showed simultaneous inhibition of C-Met with 3 monoclonal antibodies; however, despite the established antibody-based inhibition of C-Met, the detailed mechanism of affinity interaction and interaction sites of antibodies with corresponding target proteins have not yet been elucidated.

The discovery of aptamers that specifically bind to rat CD4 receptor but not to human CD4 proteins[12,13] initiated high interest in exploring aptamers as therapeutic agents. Aptamers are single stranded DNA or RNA oligonucleotides[14–16] that exert pronounced selectivity as inhibitors of signaling pathways. In contrast to antibodies, aptamers are obtained by *in vitro* selection and optimization procedures (SELEX: "**S**ystematic **E**volution of **L**igands by **EX**ponential Enrichment");[15,16] they are chemically synthesized and show a number of unique features in the development of bioassays, drug development, and targeted therapy.[15] As "chemical antibodies", aptamers are non-immunogenic and do not interfere with cell viabilities, since they specifically bind and release cells,[13] suggesting high potential for the evaluation of biomarkers. Thus, aptamers may reveal a number of advantages compared to antibodies, such as fast and easy production, high stabilities and high binding strength.[17–19]

In the present study we have pursued a new approach to elucidate the inhibiting mechanism(s) of C-Met by identifying the molecular binding sites between C-Met protein and aptamers, with the rationale to explore their binding properties and possible similarities with antibodies. Here, we report the identification of the interaction epitopes of C-Met with two DNA aptamers (CLN0003 and CLN0004) that bind to C-Met with high affinity and specificity (Figure 1; s. Table 1). Corresponding aptamers (CLN0003 and CLN0004 and analogous oligonucleotide sequences) have shown high affinity binding to C-Met and have recently gained high interest in their development for cancer therapy.[20–24] For the identification of aptamer epitopes of C-Met and determination of binding affinities, selective proteolytic extraction of C-Met-aptamer complexes in combination with electrospray (ESI) and MALDI mass spectrometry, and SPR (surface plasmon resonance) biosensor analysis were used as principal tools (PROTEX-SPR-MS)[25,26] (Supplementary Figure S1). The PROTEX-SPR-MS method has been successfully applied in a number of recent studies for epitope identifications of protein-antibody complexes, protein-peptide interactions, and carbohydrate-protein complexes.[26–32] SPR determinations of the C-Met-aptamer complexes revealed high affinities, consistent with the suitability of aptamers as specific inhibitors of C-Met. PROTEX-MS using immobilized aptamer affinity-matrices revealed specific epitopes on C-Met, with a linear epitope peptide identified for the CLN0004 aptamer, and a discontinuous epitope comprising two specific peptides for the CLN0003 aptamer. Structure modeling of the two aptamers was found to be consistent with the identified epitopes. Binding curves obtained in affinity studies suggested a conformational change following a first binding event of the aptamers, resulting in a discrete second high affinity binding step. These results show that aptamers bind to C-Met with high affinities exerting specific epitopes that may be promising biomarker candidates for cellular diagnostics.

Table 1. Sequences of the DNA aptamers CLN0003 and CLN0004.

DNA Aptamer	Sequence
CLN0003	5′-/5AmMC12/GGA GGG AAA AGT TAT CAG GCT GGA TGG TAG CTC GGT CGG GGT GGG TGG GTT GGC AAG TCT-3′
CLN0004	5′-/5AmMC12/GAG TGC CTA ATG GTA CGA TTT GGG AAG TGG CTT GGG GTG GGA TTA GTT GAG TAC TCG CTC-3′

© 2019 Wiley-VCH Verlag GmbH & Co. KGaA, Weinheim

Results and Discussion

Affinity analysis of C-Met-aptamer complexes reveals discrete interaction steps

Affinity determinations of the aptamer complexes with the C-Met protein were carried out by SPR analysis on self-assembled monolayer (SAM) gold chips, by immobilization of both the aptamers and recombinant C-Met protein (s. Experimental Section) on the chip surface using standard SAM technology (Figures S2A, B). Binding constants K_D were determined using dilution series of aptamers and the protein, respectively. The reference channel of the dual-channel detector was used to subtract unspecific interactions in the data analysis. SPR analyses of the C-Met interaction with both aptamers were performed by immobilization of aptamers and binding of a dilution series of the protein, as illustrated in Figure 2 by the interaction of CLN0004 with C-Met. Affinity determinations using the kinetic method revealed a K_D of 0.223 μM for the CLN0003 aptamer and a K_D of 0.535 μM for the CLN00004 aptamer (Table 2).

A second series of SPR determinations was performed by immobilization of the C-Met protein and provided additional information compared to the aptamer immobilization. When C-Met was immobilized on the chip surface and the analysis carried out with a dilution series of the aptamers, two discrete interaction steps were observed, suggesting different possible binding sites. Due to the imperfect shape of the curve after subtraction of the reference channel, the analyses were performed using the affinity/EC50 method, providing a K_D of 56.34 nM for the CLN0003 interaction, and 92.71 nM for CLN0004 (Figures S3 and S4). The interaction of CLN0003 with C-Met was analyzed with three different approaches: (i), determination of K_D using a one to one kinetic model of interaction sites; (ii), analysis of the sensorgram using the same kinetic measurement with a one to two interaction model; and (iii), affinity analysis and separate determination of K_D for the second binding step. The second binding event was observed after approximately one minute and the reference channel subtracted here as well. The same procedure was used for the CLN0004 aptamer and provided similar results. These results (summarized in Table S1) suggested that upon a first interaction step of the aptamer, the aptamer-protein complex undergoes a conformational modification that allows a second interaction step to occur. According to this analysis, the CLN0003 aptamer undergoes a first interaction event for about one minute, followed by a second stronger interaction. These determinations provided K_Ds of 2.0 μM (K_D1) and 0.04 μM (K_D2) for CLN0003, and 0.1 μM (K_D1) and 0.05 μM (K_D2) for the CLN0004 aptamer (Table S1).

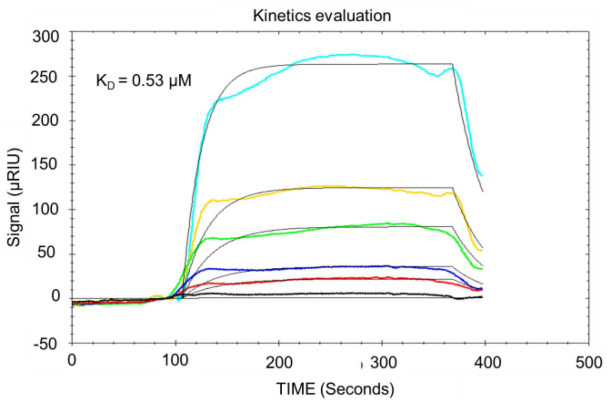

Figure 2. SPR Sensorgram for the CLN0004 – C-Met interaction complex, at a one-to-one evaluation of the complex with the aptamer immobilized and the C-Met ligand. The K_D determination yielded 0.535 μM.

Table 2. K_D determinations of CLN0003 and CLN0004 complexes with C-Met protein.

DNA Aptamer immobilized on SAM coated chip	Calculated K_D (M) from C-Met dilution series
CLN0003	2.23e-7
CLN0004	5.35e-7

Specific epitope peptides identified for C-Met-aptamer complexes

In order to obtain molecular epitope identifications, proteolytic epitope extraction mass spectrometry (PROTEX-MS) was performed as illustrated in Figure S1.[31,32] Prior to digestion, the protein was subjected to reduction of disulfide bonds and subsequent alkylation with iodoacetamide as described in the Experimental Section, followed by digestion with trypsin, and proteolytic fragment mixtures were characterized by mass spectrometric peptide mapping.

MALDI-MS analyses of C-Met with trypsin at conventional conditions (18 h; 37 °C) and at high pressure (approx. 30 kpsi; 50 min) are compared in Figure 3. In both cases digestion yields >90% were obtained providing nearly complete sequence coverage. However, high pressure digestion was found to provide substantially faster degradation, associated with a cleaner fragmentation pattern (lower background). Moreover, improved reproducibility was found regarding the detection of low abundance fragments.

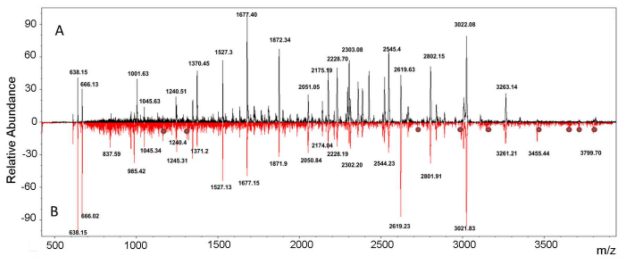

Figure 3. MALDI-MS analysis of trypsin digestion mixture of C-Met protein at standard conditions (18 h, 37 °C) (A), and high pressure using the Barocycler 2320EXT (Pressure Biosciences; 50 min, 25 °C) (B). Additional tryptic fragments identified at high pressure digestion are marked with red dots.

© 2019 Wiley-VCH Verlag GmbH & Co. KGaA, Weinheim

Epitope determinations were performed with aptamers immobilized on Sepharose microaffinity beads, using two complementary approaches as previously described[30,32] (Figure S1): (a), Proteolytic epitope extraction following aptamer immobilization on a Sepharose microaffinity column; (b), Epitope extraction and MALDI-MS following immobilization of aptamers on the SPR chip and subsequent elution. Following removal of supernatant peptides by washing with aqueous solvent, no background peptide was observed in the last washing fraction, and elution was subsequently performed with slightly acidified solvent (0.1 % TFA).

MALDI-MS analyses of the elution fractions from tryptic epitope extraction of C-Met from the CLN0004 aptamer affinity column, and elution from the aptamer-SPR chip are shown in Figures 4A, and B. Both approaches yielded identical results with most abundant singly charged epitope peptide ions, r.NSSGC(carbamidomethyl)EAR.r at m/z 881.45 (C-Met(381–388)), protonated MH^+ and Na^+ and K^+ molecular adduct ions. In the elution fraction from the affinity microcolumn, an additional smaller peptide was found at m/z 800.4 and identified as RDEYR (389–393). The identical epitope peptide sequence (381–388) was found upon elution from the SPR chip. These results provided evidence of a single linear epitope peptide, NSSGCEARRDEYR (381–393), for the CLN0004 aptamer. Additional confirmation of the epitope was obtained by CID (collision-induced-dissociation)-tandem-MALDI-MS (data not shown). Notably, the R389 residue was found uncleaved by trypsin, indicating shielding of the epitope in the aptamer interaction (s. Table 3).

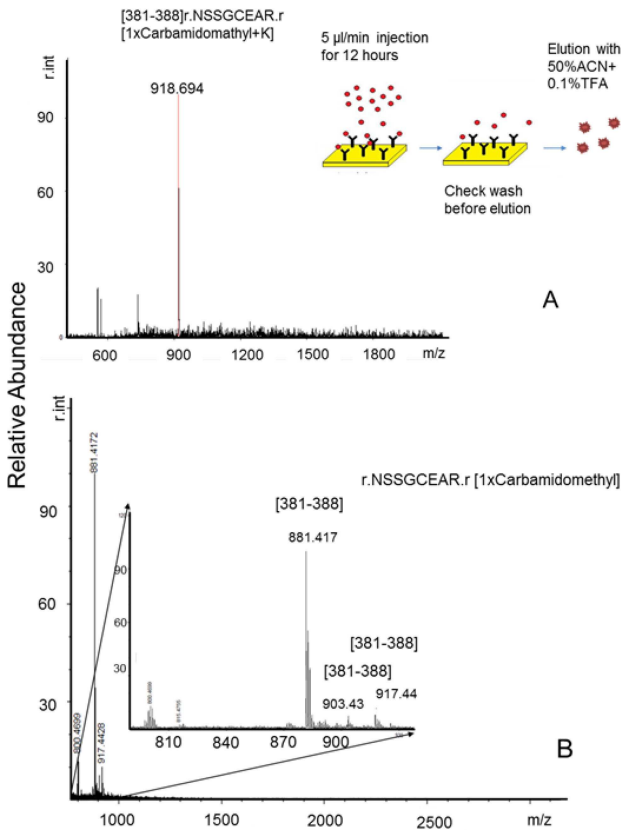

Figure 4. A) Tryptic epitope extraction-MS from immobilized CLN0004 aptamer on SAM coated SPR chip. B) Epitope extraction-MS from immobilized CLN0004 aptamer on CNBr-activated Sepharose affinity matrix.

In contrast to the CLN0004 aptamer, the epitope analysis of the C-Met complex with the CLN0003 aptamer provided two epitope peptides within adjacent structure domains, C-Met (524–543) and C-Met (568–576), (SEECLSGTWTQQICLPAIYK) and (NNKFDLKK), respectively (Table 3 and Figure S5). In this discontinuous (conformational) epitope, the residues K570 and K574 of the peptide C-Met(568–576) were found uncleaved and thus shielded from proteolytic digestion. This structural information of the binding site of the CLN0003 aptamer is of considerable interest since previous studies indicated that CLN0003 is interfering with the interaction of the growth factor HGF with C-Met,[37] suggesting the possible application of this aptamer as an inhibitor. The epitope identification was further ascertained by partial tryptic digestion in a proteolytic epitope excision experiment of the intact C-Met/aptamer complex and molecular weight filtration. The C-Met-aptamer complex was incubated with trypsin for 4 hours; the digestion solution was then passed through a 10 kDa molecular weight cutoff filter, subjected to centrifugation and washed with an excess volume of ammonium bicarbonate. MALDI-MS analysis of the epitope fraction eluted from the aptamer complex provided a major polypeptide at m/z 6139.9, C-Met (489–543), comprising the epitope peptide (524–543) (Figure S6). In the epitope peptide sequence, the residues R523 and K520 were found shielded from tryptic digestion.

Synthetic C-Met epitope peptides reveal high affinities

The tryptic epitope peptides of the aptamers CLN0003 and CLN0004 binding to the C-Met protein (NSSGCEAR; NNKFDLKK; SEECLSGTWTQQICLPAIYK) were synthesized by SPPS on a preloaded PS-PHB resin. Primary structures and homogeneities of the peptides were confirmed by mass spectrometry, and indicated >90 % purities (s. Figure S7). Affinities and binding constants of the aptamer-peptide complexes were determined on SAM-SPR chips by immobilization of aptamers, and K_D values of 30–100 µM were obtained in first affinity experiments. Affinities of the epitope peptides were found considerably lower compared to intact C-Met; however, the specificities of the epitopes were confirmed by affinity-MS experiments with proteolytic peptide mixtures of C-Met, which showed only epitope peptides in the affinity-eluate fractions.

Table 3. Epitope peptides identified for aptamer CLN0003 and CLN0004 interactions with the C-Met protein. K and R residues in the epitope peptides shielded from digestion are marked in bold.

Aptamer	C-Met epitope peptide	Sequence
CLN0003	SEECLSGTWTQQICLPAIYK	(524–543)
CLN0003	NN**K**FDL**K**K	(567–575)
CLN0004	NSSGCEAR**R**DEYR	(381–393)

© 2019 Wiley-VCH Verlag GmbH & Co. KGaA, Weinheim

Conclusions

In this study we present the molecular identification and affinity determination of specific epitope peptides of the C-Met protein binding to two high affinity aptamers, using proteolytic epitope extraction mass spectrometry, in combination with SPR biosensor analysis (PROTEX-SPRMS). The identified epitopes were found to be localized at distinct binding sites within the C-Met structure. Size and location of the epitopes and structure modeling of the C-Met complexes with the aptamer epitopes suggest that the structural requirements of epitope binding to aptamers are generally comparable to binding sites within the variable paratope regions of antibodies. Affinities of the aptamers determined by SPR were similar to those previously reported for C-Met aptamers with comparable sequences using dot blot/radioactive labeling and phosphorimaging, despite the different methodologies used.[22,23] Molecular structure modeling of the CLN0003 and CLN0004 aptamers, was performed by the Avogadro software package, using the Mfold web server for prediction of nucleic acid folding and hybridization,[38,39] and molecular docking studies of the aptamer-C-Met complexes performed using the AutoDock 4.0 software package as described in the Experimental Section (Figure 5; Figures S8, S9). The affinity determinations of the aptamers with C-Met suggest two distinct binding events, both by the observed SPR analyses and the corresponding data processing. For the CLN0003 aptamer a first interaction was found to be about 100 times weaker than the second, while for the CLN0004 aptamer the second interaction was found approximately 10 times stronger than the first interaction, consistent with a single linear epitope sequence of this aptamer.

The molecular identification of specific aptamer epitopes to C-Met, determined here for the first time by mass spectrometry, should be of considerable interest for future drug development studies with aptamers. Although C-Met antibodies have been admitted to first clinical trials, recent studies indicate considerable difficulties in the development of inhibiting antibodies with high stability and specificity.[21,22] Except for the monoclonal antibody Onortuzumab that inhibits binding to HBF, no antibody has been described inhibiting the C-Met interaction with HGF. Major problems for the development of antibodies may be encountered by difficulties in antibody delivery, and by the possible formation of immunogenic anti-drug antibodies.[22,23] These problems could be efficiently tackled with aptamers. In addition to their high stability and binding reproducibility, aptamers are shown here to bind with high affinity and specificity. Moreover, aptamers generally should have low immunogenicity.[35] Thus, the structure-based binding specificity and affinity of aptamers should render their molecular development and characterization an attractive alternative to antibodies.

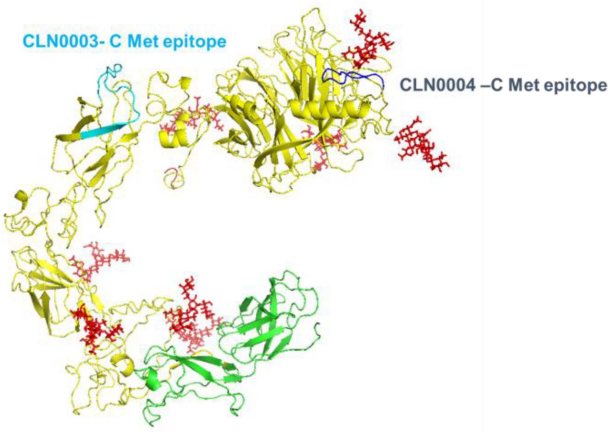

Figure 5. Structure modeling for C-Met complexes with CLN0003 (light blue) and CLN0004 aptamer epitope peptides (dark blue) at the epitope binding sites in the structures selected with the lowest docking energy the aptamer epitope ligands are shown with green balls, and the C-Met with blue balls.

Experimental Section

DNA aptamers

The C-Met specific DNA aptamer sequences CLN0003 and CLN0004 were produced by IDT Integrated DNA Technologies (Coralville, Iowa, USA) based on the published aptamers.[22] The aptamers were produced using the filter SELEX procedure with a recombinant C-Met protein, and were tested on C-Met-positive cell lines GTL-16, MKN-45, and EBC-1. The C-Met aptamers CLN0003 and CLN0004 consisting of 60 and 64 bases were synthesized with an amino group (5AmMC12) on the 5′end, respectively (s. Table 1). Affinities determined by SPR were similar to those previously reported for C-Met aptamers with comparable sequences.[23]

Preparation and characterization of C-Met

Human recombinant C-Met protein with C-terminal His and Fc Tags was obtained from Sino Biologicals (Wayne, PA; USA; Cat-No. 10692-H03H). A DNA sequence encoding the extracellular domain (Met1–Thr932) of human C-Met (NCBI Reference Sequence: NP_000236) was fused with the C-terminal polyhistidine-tagged Fc region of human IgG1 at the C-terminus. Molecular weight and sequence homogeneity of the C-Met was confirmed by MALDI-MS.

Proteolytic digestion

A stock solution of 1 mg/mL C-Met protein in MilliQ water was prepared for proteolytic digestion. Prior to digestion the C-Met protein was reduced and alkylated. For reduction of disulfide bonds four aliquots (10 μg each) of C-Met were diluted in 15 μL ammonium hydrogen carbonate (100 mM, pH 7.6) and incubated for 15 min at 25 °C with 5 μL 6 M guanidine-HCl and 1.5 μL reduction solution (10 mM DTT). Subsequent alkylation was performed by adding 5 μL of ammonium hydrogen carbonate buffer to a 10 μg aliquot of the reduced C-Met solution, and incubation of the protein with 15 μL 100 mM iodoacetamide for 1 h at subdued light.

Tryptic digestion was performed with an enzyme : substrate ratio of 1 : 100 (enzyme to protein). Trypsin (Serva, Heidelberg, Germany) was added to two of the aliquots and the sample incubated for 18 h at 37 °C. After digestion was complete as checked by MALDI-MS, the enzymatic activity was quenched with 0.1 % trifluoroacetic acid (TFA). High pressure proteolytic digestion was performed with a Barocycler 2320EXT instrument (Pressure BioSciences; Boston/USA). The protein was dissolved in MilliQ water and aliquoted in 4

© 2019 Wiley-VCH Verlag GmbH & Co. KGaA, Weinheim

Eppendorf vials (50 μL each) at a concentration of 1 mg/mL. A aliquot of 10 μg was reduced and alkylated as described above, and 0.5 μg of Trypsin was added. The sample solution was then diluted with 30 μL 10 mM ammonium hydrogen carbonate buffer, pH 7.6. High pressure digestion was performed at 35 kpsi for 10 min (on), 1 min (off) for 5 cycles at 20 °C. A total digestion time of 50 min was used, and analysis of digest mixtures performed by MALDI-MS. MALDI-MS Analyses were performed with a Bruker Autoflex III Smartbeam-MS (Bruker Daltonics, Bremen, Germany).[31,32] All digestion mixtures were further characterized by gel electrophoresis; proteolytic peptide mixtures provided digestion yields > 95 % and were used for epitope analyses.[32]

Preparation of affinity microcolumns

Affinity microcolumns with NHS/EDC-activated Sepharose beads were prepared with 20 mg of Sepharose incubated with 0.1 M HCl for 15 min and washed with coupling buffer (0.2 M sodium hydrogen carbonate + 0.5 M NaCl, pH 8). An aliquot of 75 μg of aptamer with a 5′ amino group was added to each column and incubated with shaking for 3 hours.

The affinity column was then blocked with 0.2 M ethanolamine + 0.5 M NaCl, pH 8.3, washed three times with washing buffer (0.2 M NaOAc + 0.5 M NaCl, pH 4), and then resuspended in ammonium hydrogen carbonate buffer, pH 7.5. Affinity columns were stored at 4 °C until use.

Epitope identification

Epitope analysis was carried out by epitope-extraction mass spectrometry, as previously described.[29,30] Briefly, 10 μg of the tryptic digestion mixture was incubated with the CLN0003 aptamer affinity column. An aliquot digest mixture of 10 μg was incubated in the same manner with the CLN0004 aptamer. Identical procedures of epitope identification were used for both aptamer affinity columns. After incubating the proteolytic mixtures for 2 h, the column was washed with 5 mL ammonium bicarbonate buffer, pH 7.5, until no background signal was observed by MALDI-MS. The epitope fraction was then eluted with 100 μL 0.01 % TFA, pH 2.5, and the eluate analyzed by MALDI MS. Following MS analysis the column was resuspended in ammonium bicarbonate buffer.

Synthesis of epitope peptides

Fmoc protected amino acid derivatives were obtained from Novabiochem (Heidelberg, Germany). N,N′-dimethylformamide (DMF), N-methyl-2-pyrrolidone (NMP), dichloromethane (DCM), (2-(1H-Benzotriazol-1-yl)-1,1,3,3-tetramethyluronium-hexafluoro-phosphate (HBTU), diisopropyl-ethylamine (DIPEA) and trifluoracetic acid (TFA) were purchased from Applied Biosystems (Darmstadt (Germany); piperidine was obtained from Acros Organic and triisopropylsilane (TIS) from Alfa Caesar (Bonn, Germany). Fmoc Solid phase peptide synthesis (Fmoc-SPPS) was carried out with an automated peptide synthesizer ABI-433A from Applied Biosystems (Darmstadt, Germany). Epitope peptides (H-NSSGCEAR, H-LTICGWDFGFRR, and H-SEECLSGTWTQQICLPAIYK) were synthesized on preloaded PS-PHB resins from RAPP-Polymer (Herrenberg, Germany) with the corresponding amino acids of the C-terminus (PS-PHB-Arg(PMC)-Fmoc, capacity 0.59 mmol/g and PS-PHB-Lys (Boc)-Fmoc, capacity 0.55 mmol/g). A standard synthesis for 0.1 mmol of each peptide was performed with the Fmoc protected amino acids. Side chain protection and removal of peptides from the resin were carried out by incubating the resin for 1 h in 5 mL of 94 % TFA, 3 % TIS and 3 % MilliQ water. The peptide was then precipitated into 20 mL diethyl ether, centrifuged and the diethyl ether decanted. Purification of the crude peptides was performed by HPLC (2795 alliance HT instrument, Waters) and a C18 column (250 × 4.6 mm, Varian SN 0976069). Characterization of peptides for molecular homogeneity was carried out by ESI-MS (Waters Quattro-Ultima III; Manchester, UK).

Molecular weight cutoff filtration after epitope excision

For epitope identification in solution, 10 kDa molecular weight cutoff filters were used (Amicon; Merck Science Research, Darmstadt, Germany). The proteolytic peptide mixture resulting from trypsin digestion of intact C-Met-aptamer was added to the Amicon filter, and 300 ul ammonium hydrogen carbonate buffer (pH 8) added to remove unbound peptides. The filter was then centrifuged for 20 min at 10,000 rpm with a Heraeus Biofuge 13 (Marshall Scientific Inc., Hampton, New Hampshire, USA). The washing step was repeated 4 times to ensure that the isolated sample consisted only of the aptamer associated with the epitope. The epitope peptide was then dissociated from the aptamer by acidification by the MALDI matrix (2 mg/mL of 2.5 dihydrobenzoic acid in 50 % ACN with 0.1 % TFA), and analyzed by MALDI-MS.

Affinity determinations of C-Met-aptamer interactions

SPR Determinations were performed with an Ametek-Reichert 2Ch7500 SPR instrument (Ametek, Buffalo, N.Y., USA), using glass slides of 0.9 mm (1 × 1 cm gold chips with a 40 nm gold layer, prepared at the Institute for Microtechnologies, Rhein-Main University, Rüsselsheim am Main, Germany). Immobilization of C-Met on the SPR chips was carried out with a solution of 200 μg/mL protein in PBS. Preparation of activated SAM chips was performed with a mixture of 200 mM *N*-(3-dimethylaminopropyl)-*N*-ethylcarbodiimide (EDC) and 50 mM *N*-hydroxysuccinimide (NHS), followed by injection of 50 μg protein in 250 μL 10 mM sodium acetate buffer, pH 5.5. Remaining free NHS reagent was then blocked with 1 M ethanolamine, pH 8.5.

Affinity determinations were carried out after immobilization of the protein as described above. A repetitive sequence of seven injections of 250 μL of aptamer solution was performed at different concentrations (80 nM–1.04 μM for CLN0003; 78 nM–10 μM for CLN0004 aptamer), at a flow rate of 25 μL/min. All SPR determinations were performed in 10 mM PBST buffer, pH 7.5 at 20 °C. K_D values were determined by applying fitting models (i), to a One-To-One interaction model, (ii), a One-To-Two model, and (iii), by affinity determination using the TraceDrawer 1.7.1 software package.[36] SPR Determinations of synthetic epitope peptides were performed in the same manner, by preparation of dilution series of peptides at concentration ranges of 600 nM–3.5 μM (s. Table S1).

Molecular docking of C-Met-aptamer complexes

Secondary structure modeling was performed using the Mfold web server for nucleic acid folding and hybridization prediction.[38] The structures of the aptamers were built by the Avogadro software package,[39] and structure models optimized using the fragment molecular orbital (FMO) method at the level of two-body FMO expansion.[40,41] Docking studies of orientation and binding sites of the aptamer-C-Met complexes were performed using the AutoDock 4.0 software package (www://autodock.scripps.edu).[42] The selected structures with the lowest docking energy of the aptamer are shown in Figure 5. Ligands are presented as blue bolls, and DNA aptamer is shown as green bolls.

© 2019 Wiley-VCH Verlag GmbH & Co. KGaA, Weinheim

Acknowledgements

We gratefully acknowledge the advice and assistance of Prof. Friedemann Völklein and Oliver Müller, MSc in the preparation of chips for the SPR affinity determinations. We thank Dr. Stefan Maeser, Biogen GmbH, München, for valuable advice and critical reading of the manuscript. This work has been partially funded (Chip-MS epitope analysis) by the LOEWE-3 Funding Agency, Hessen-Agentur, Wiesbaden, Germany; Grant 696/19-16.

Conflict of Interest

The authors declare no conflict of interest.

Keywords: C-Met protein · tumor biomarkers · aptamer-C-Met complexes · aptamer epitopes · affinity-mass spectrometry · epitope peptide analysis

[1] S. L. Organ, M. S. Tsao, *Ther. Adv. Med. Oncol.* **2011**, *3*, 7–19.
[2] C. G. Huh, V. M. Factor, A. Sánchez, K. Uchida, E. A. Conner, S. S. Thorgeirsson, *Proc. Nat'l Acad. Sci. USA* **2004**, *101*, 4477–4482.
[3] J. Stamos, R. A. Lazarus, X. Yao, D. Kirchhofer, C. Wiesmann, *EMBO J.* **2004**, *23*, 2325–2335.
[4] A. Gentile, L. Trusolino, P. M. Comoglio, *Cancer Metastasis Rev.* **2008**, *27*, 85–94.
[5] N. Rahimi, E. Tremblay, L. McAdam, M. Park, R. Schwall, B. Elliott, *Cell Growth Differ.* **1996**, *7*, 263–270.
[6] N. Horiguchi, H. Takayama, M. Toyoda, T. Otsuka, T. Fukusato, G. Merlino, H. Takagi, M. Mori, *Oncogene.* **2002**, *21*, 1791–1799.
[7] P. Hyunkyu, K. Donggeon, S. Eunju, S. Sunhwa, K. S. Jason, K. Seok-Hyung, Y. Yeup, N. Do-Hyun, *Biochem. Biophys. Res. Commun.* **2017**, *494*, 409–415.
[8] N. Sharma, A. A. Adjei, *Ther. Adv. Med. Oncol.* **2011**, *3*, S37–S50.
[9] J. S. Wong, E. Warbrick, B. Vojtesek, J. Hill, D. P. Lane, *Oncotarget.* **2013**, *4(7)*,1019–1036.
[10] B. Cao, Y. Su, M. Oskarsson, P. Zhao, E. J. Kort, R. J. Fisher, L. M. Wang, G. F. Vande Woude, *Proc. Natl. Acad. Sci. USA.* **2001**, *98*, 7443–7448.
[11] H. Ki, H. Kimand, *Exp. Mol. Med.* **2017**, *49*, e308.
[12] A. Nozari, M. V. Berezovski, *Mol. Ther. Nucleic Acids* **2017**, *6*, 29–44.
[13] T. N. Zamay, G. S. Zamay, O. S. Kolovskaya, R. A. Zukov, M. M. Petrova, A. Gargaun, M. V. Berezovski, A. S. Kichkailo, *Cancers* **2017**, *9*, 155.
[14] F. Pastor, M. M. Soldevilla, H. Villanueva, D. Kolonias, S. Inoges, A. L. de Cerio, R. Kandzia, V. Klimyuk, Y. Gleba, E. Gilboa, M. Bendandi, *Mol. Ther. Nucleic Acids.* **2013**, *2*, e98.
[15] Y. Zhang, B. S. Lai, M. Juhas, *Molecules* **2019**, *24*, 941.
[16] A. S. Zamay, G. S. Zamay, O. S. Kolovskaya, T. N. Zamay, M. V. Berezovski, *Springer.* **2017**, Vol. 994.
[17] Z. Zhao, L. Xu, X. Shi, W. Tan, X. Fang, D. Shangguan, *Analyst (Lond.).* **2009**, *134*, 1808–1814.
[18] Y. Song, Z. Zhu, Y. An, W. Zhang, H. Zhang, D. Liu, C. Yu, W. Duan, C. J. Yang, *Anal. Chem.* **2013**, *85*, 4141–4149.
[19] H. W. Chen, C. D. Medley, K. Sefah, D. Shangguan, Z. Tang, L. Meng, J. E. Smith, W. Tan, *ChemMedChem.* **2008**, *3*, 991–1001.
[20] T. Kunii, S. Ogura, M. Mie, E. Kobatake, *Analyst (Lond.)* **2011**, *136*, 1310–1312.
[21] G. S. Zamay, T. I. Ivanchenko, T. N. Zamay, V. L. Grigorieva, Y. E. Glazyrin, O. S. Kolovskaya, I. V. Garanzha, A. A. Barinov, A. V. Krat, G. G. Mironov, A. Gargaun, D. V. Veprintsev, S. S. Bekuzarov, A. K. Kirichenko, R. A. Zukov, M. M. Petrova, A. A. Modestov, M. V. Berezovski, A. S. Zamay, *Mol. Ther. Nucleic Acids.* **2017**, *6*, 150–162.
[22] A. Boltz, B. Piater, L. Toleikis, R. Guenther, H. Kolmar, B. Hock, *J. Biol. Chem.* **2011**, *286*, 21896–21905.
[23] B. Piater, A. Doerner, R. Guenther, H. Kolmar, B. Hock, *PLoS One* **2015**, *10 (12)* e0142412.
[24] J. G. Bruno, *Molecules.* **2015**, *20*, 6866–6887.
[25] B. A. Petre, M. Ulrich, M. Stumbaum, B. Bernevic, A. Moise, G. Döring, M. Przybylski, *J. Am. Soc. Mass Spectrom.* **2012**, *23*, 1831–1840.
[26] A. Moise, S. André, F. Eggers, M. Krzeminski, M. Przybylski, H. J. Gabius, *J. Am. Chem. Soc.* **2011**, *133*, 14844–14847.
[27] J. McLaurin, R. Cecal, M. E. Kierstead, X. Tian, A. L. Phinney, M. Manea, J. E. French, M. L. H. Lambermon, A. A. Darabie, M. E. Brown, C. Janus, M. A. Chishti, P. Horne, D. Westaway, P. E. Fraser, M. T. J. Mount, M. Przybylski, P. St.-George-Hyslop, *Nat. Med.* **2002**, *8*, 1263–1269.
[28] R. Stefanescu, R. E. Iacob, E. N. Damoc, A. Marquardt, E. Amstalden, M. Manea, I. Perdivara, M. Maftei, G. Paraschiv, M. Przybylski, *Eur. J. Mass Spectrom.* **2007**, *13*, 69–75.
[29] P. Juszczyk, G. Paraschiv, A. Szymanska, A. S. Kolodziejczyk, S. Rodziewicz-Motowidlo, Z. Grzonka, M. Przybylski, *Simulation, J. Med. Chem.* **2009**, *52*, 2420–2428.
[30] M. I. Iurascu, O. Marroquin Belaunzanar, C. Cozma, U. Petrausch, C. Renner, M. Przybylski, *J. Am. Soc. Mass Spectrom.* **2016**, *27*, 1105–1112.
[31] A. Moise, S. Maeser, S. Rawer, F. Eggers, M Murphy, J. Bornheim, M. Przybylski, *J. Am. Soc. Mass Spectrom.* **2016**, *27*, 1071–8.
[32] Z. Kukacka, M. Iurascu, L. Lupu, H. Rusche, M. Murphy, L. Altamore, F. Borri, S. Maeser, A. M. Papini, M. Przybylski, *ChemMedChem.* **2018**, *13*, 909–915.
[33] D. Lee, E. S. Sung, J. H. Ahn, J. An, S. Huh, W. K. You, *Immunotargets Ther.* **2015**, *4*, 35–44. .
[34] Trace Drawer V. 1.7.1 ; Ridgeview Instruments AB, Vänge, Sweden.
[35] A. Lakhin, V. Tarantul, L. Gening, *Acta Naturae.* **2013**, *5*, 34–43.
[36] J. Yang, R. Yan, A. Roy, D. Xu, J. Poisson, Y. Zhang, *Nat. Methods* **2015**, *12*, 7–8.
[37] R. Ueki, S. Sando, *Chem. Commun.* **2014**, *7*, 13131–13134.
[38] M. Zuker, *Nucleic Acids Res.* **2003**, *31*, 3406–3415.
[39] M. D. Hanwell, D. E. Curtis, D. C. Lonie, T. Vandermeersch, E. Zurek, G. R. Hutchison, *J. Cheminf.* **2012**, *4*, 17.
[40] D. G. Fedorov, *Comp. Mol. Sci.* **2017**, *7*, e1322.
[41] M. Gaus, A. Goez, M. Elstner, *J. Chem. Theory Comput.* **2013**, *9*, 338–354.
[42] M. Gaus, A. Goez, M. Elstner, *J. Chem. Theory Comput.* **2013**, *9*, 338–354.

Manuscript received: August 24, 2019
Revised manuscript received: November 29, 2019
Accepted manuscript online: December 11, 2019
Version of record online: January 16, 2020

© 2019 Wiley-VCH Verlag GmbH & Co. KGaA, Weinheim